CHIN. PHYS. LETT. Vol. 35, No. 2 (2018) 027701

Gap States of ZnO Thin Films by New Methods: Optical Spectroscopy, Optical Conductivity and Optical Dispersion Energy

Vali Dalouji[1**], Shahram Solaymani[2], Laya Dejam[3], Seyed Mohammad Elahi[2], Sahar Rezaee[4], Dariush Mehrparvar[1]

[1]*Department of Physics, Faculty of Science, Malayer University, Malayer, Iran*
[2]*Department of Physics, Science and Research Branch, Islamic Azad University, Tehran, Iran*
[3]*Department of Physics, West Tehran Branch, Islamic Azad University, Tehran, Iran*
[4]*Department of Physics, Kermanshah Branch, Islamic Azad University, Kermanshah, Iran*

(Received 18 September 2017)

The optical reflectance and transmittance spectra in the wavelength range of 300–2500 nm are used to compute the absorption coefficient of zinc oxide films annealed at different post-annealing temperatures 400, 500 and 600°C. The values of the cross point between the curves of the real and imaginary parts of the optical conductivity σ_1 and σ_1 with energy axis of films exhibit values that correspond to optical gaps and are about 3.25–3.3 eV. The maxima of peaks in plots $dR/d\lambda$ and $dT/d\lambda$ versus wavelength of films exhibit optical gaps at about 3.12–3.25 eV. The values of the fundamental indirect band gap obtained from the Tauc model are at about 3.14–3.2 eV. It can be seen that films annealed at 600°C have the minimum indirect optical band gap at about 3.15 eV. The films annealed at 600°C have Urbach's energy minimum of 1.38 eV and hence have minimum disorder. The dispersion energy E_d of films annealed at 500°C has the minimum value of 43 eV.

PACS: 77.55.hf, 78.66.Bz, 78.68.+m DOI: 10.1088/0256-307X/35/2/027701

Amongst different metal oxides, probably zinc oxide has the most different nano-shapes comprised of nano-wires, nano-rods, hollow nano-spheres, colloidal nano-particles and nano-tube, which are still under intensive research.[1–3] Many researchers have been devoted to studying zinc oxide and doping with a variety of elements, such as Al, Ga, and In to improve their properties for various applications.[4,5] The properties of zinc oxide were also modified enormously by introducing a variety of defects such as annealing in Ar, N_2, O_2, and H_2 atmospheres affecting various properties of zinc oxide films depending on the sort of defects introduced to films.[6–9] In the previous reports we studied the effect of deposition times, deposition rate, and annealing temperature on the structural and optical properties with emphasis on absorption coefficients and the Wemple–Didomenico dispersion (WDD) parameters in carbon films embedded by nickel.[10–19] In this Letter, we study the optical gaps using different methods and the WDD parameters of zinc oxide films at different post-annealing temperatures in Ar atmosphere.

ZnO films were synthesized on quartz substrates by radio-frequency magnetron sputtering. Sputtering gas was Ar and O_2 with the $O_2/(O_2+Ar)$ ratio of 30% and remained constant during operation by employing two rotary and turbo pumps. Power of sputtering was 125 W for deposition of ZnO films. Base pressure was 2×10^{-4} mbar and initial vacuum for sputtering was 7.8×10^{-3} mbar. The target was sputtered for 30 min to remove any possible oxide. Zn metal target was a disk with diameter of 77 mm and thickness of 3 mm of Zn in purity of 99.99 % melted at 600℃ to reach the Zn target. Thickness of deposited films was 230±5 nm as measured by a quartz crystal monitor during deposition. A DEKTAK 3 profilometer was employed for measuring the thickness after deposition. Annealing was carried out in a furnace by argon flux at three different temperatures of 400, 500 and 600℃ for 1 h with the rate of 10℃/min. Optical measurements were performed by a Varian Cary-500 spectrophotometer in the range of 200–2500 nm (Varian Inc., CA, USA). Topology and RMS roughness of thin films were determined by Veeco Autoprobe in contact mode. All measurements were made at room temperature.

Figure 1(a) shows the optical absorption coefficients of the films as a function of the incident photon wavelength. With the post-annealing temperature increasing from 300 to 500℃, optical absorption coefficients of the films decrease and then from 500 to 600℃ they increase. Figure 1(b) shows the variation of mean height of nano-particle size of films as a function of the annealing temperature. Increasing post-annealing temperature of films causes to increase the size of nano-particles obtained from AFM analyses. The size of nano-particles in the as-deposited films and in the films annealed at 500℃ increases from about 17 to 32 nm. The large grain sizes result in larger unfilled inter-granular volume, thus the absorption per unit thickness is decreased.[20,21] It can be seen that with increasing the post-annealing temperature from 500 to 600℃ the optical absorption coefficients of the films increase. The size of nano-particles in the films from 500 to 600℃ decreases nearly from 32 to 28 nm. The small grain sizes result in smaller unfilled inter-

**Corresponding author. Email: dalouji@yahoo.com
© 2018 Chinese Physical Society and IOP Publishing Ltd

granular volume, thus the absorption per unit thickness is increased. Figures 1(c) and 1(d) show the typical AFM images of films annealed at 400℃ and 500℃, respectively.

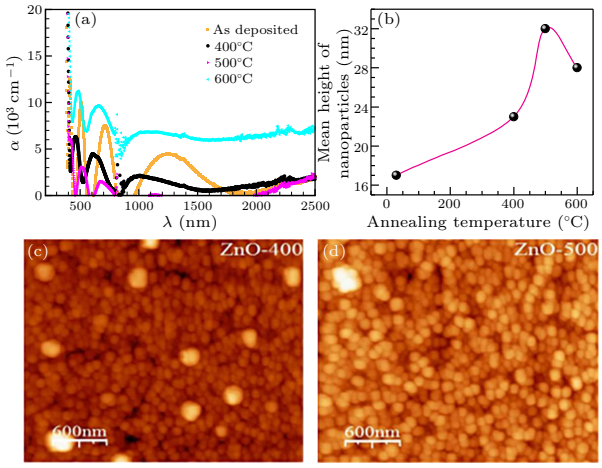

Fig. 1. (a) Variation of absorption coefficient spectra of films as a function of the incident photon wavelength. (b) Variation of nanoparticle size on surface of films with annealing temperature and typical AFM images of films annealed at 400℃ (c) and 500℃ (d).

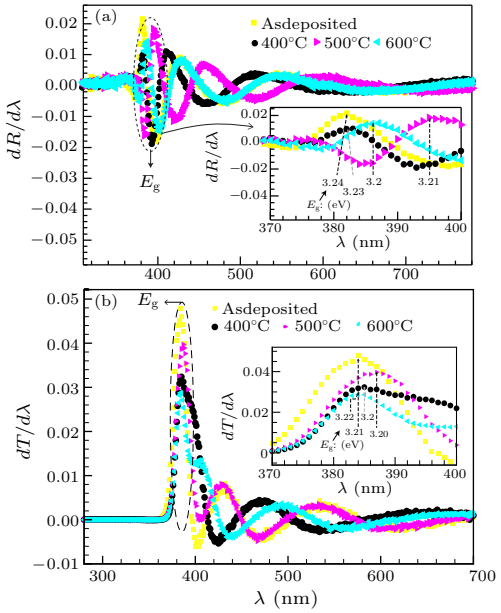

Fig. 2. Variations of $dR/d\lambda$ (a) and $dT/d\lambda$ (b) of the films as a function of the incident photon wavelength. Insets: variation of these plots versus the incident photon wavelength in the optical band gap of films.

Figures 2(a) and 2(b) show the variation of plots $dR/d\lambda$ and $dT/d\lambda$ of films as a function of the incident photon wavelength, respectively. These plots are applied for estimating the absorption band edge of the films. As seen in these figures, the position of the peak maximum corresponds to the absorption band edge.[22] As shown in Fig. 2(a), the optical band gap lies in the range of 3.12–3.25 eV, and as shown in Fig. 2(b) the optical band gap lies in the range of 3.19–3.22 eV. There is a remarkable effect for post-annealing temperature in the studied range on the optical band gap estimated from $dR/d\lambda$ and $dT/d\lambda$ versus wavelength. The optical band gap estimated from $dR/d\lambda$ and $dT/d\lambda$ versus wavelength, suggesting that the optical band gap of films up to 500℃ shifts from 3.24 to 3.12 eV and over 500℃ it shifts from 3.12 to 3.25 eV. The increasing nano-particle size from 17 to 32 nm at 500℃ causes red shift and then the decreasing nanoparticle size from 32 to 28 nm in the films annealed from 500 to 600℃ causes blue shift in these plots. Therefore, these red and blue shifts can be due to the quantum size effect.

The complex optical conductivity σ^* ($\sigma^* = \sigma_1 + i\sigma_2$) is related to the complex dielectric constant ε^* ($\varepsilon^* = \varepsilon_1 + i\varepsilon_2$).[23] Figure 3 shows the variations of σ_1 and σ_2 with the photon energy for films with different post-annealing temperatures from 400 to 600℃. It is clear that the real part decreases with increasing the photon energy while the imaginary part increases with the photon energy. Values of the optical band gap can be estimated from the cross point between the curves of the real and imaginary parts of the optical conductivity to the photon energy axis.

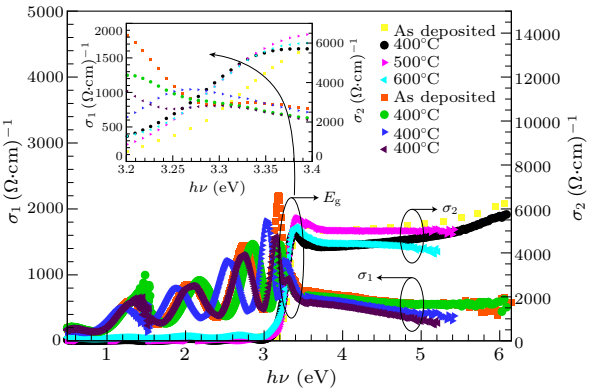

Fig. 3. Dependence of the real and imaginary parts of the optical conductivity of films as a function of the incident photon energy. Inset: variation of these plots versus the incident photon energy in the optical band gap of the films.

For the first region of the higher values of the absorption coefficient, $\alpha > 10^4\,\mathrm{cm}^{-1}$, the optical absorption edge is analyzed by the Tauc power law for the direct optical transition according to m in the equation $\alpha = (A/h\nu)(h\nu E_\mathrm{g})^m$, where A is an energy-independent constant, and E_g is the optical band gap.[24–29] This equation can be rewritten as $d[\ln(\alpha h\nu)]d(h\nu) = m/(h\nu - E_\mathrm{g})$. The type of the optical transition can be obtained to find the value of m.[30] Figure 4(a) shows the variation of $d[\ln(\alpha h\nu)]d(h\nu)$ versus $h\nu$ for the as-deposited films and post-annealing temperatures at 400, 500 and 600℃. The peak at a particular energy value gives approximately the optical band gap. This peak is found to be at about $h\nu = E_\mathrm{g} \approx 3.3$ eV, which is consistent with the band gaps obtained with different methods for the films. Figure 4(b) shows $\ln(\alpha h\nu)$ versus $\ln(h\nu - E_\mathrm{g})$ for the as-deposited films and post-

annealing temperatures at 400, 500 and 600℃. Using E_g, m is determined from the slope of Fig. 4(b).

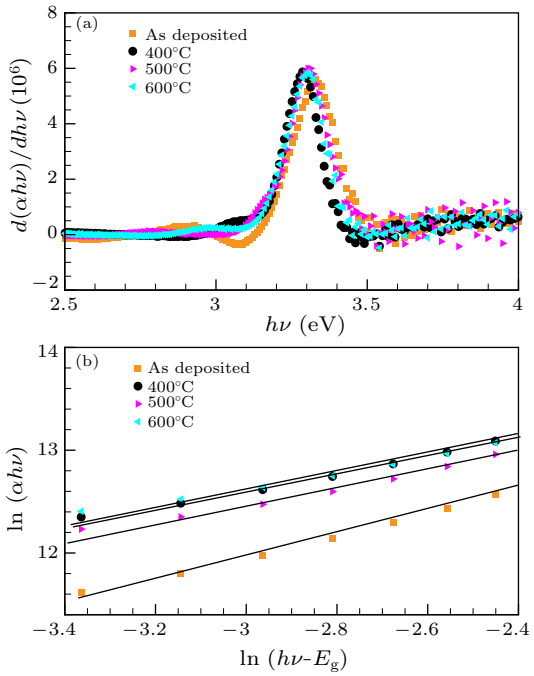

Fig. 4. Variation of $d(\alpha h\nu)/d(h\nu)$ of the films (a) versus $h\nu$ and versus $\ln(h\nu - E_g)$ (b).

Figure 5(a) shows the variation of $(\alpha h\nu)^2$ for the as-deposited films and post-annealing temperatures at 400, 500 and 600℃ as a function of the photon energy. The optical band gap is determined by extrapolating the linear portion of the plots to $(\alpha h\nu)^2 = 0$. This suggests that the fundamental absorption edge of the films is formed by the indirect allowed transitions. The calculated values of the optical band gap for the as-deposited films and post-annealing temperatures are determined, as listed in Table 1. These results are consistent with the results of particle sizes obtained from the AFM analysis, which shows that the particle sizes increase with the increasing annealing temperature. We know that due to the disordered nature of the deposited films, localized states are produced in the lowest part of the conduction band and therefore the absorption edge shifts to a higher energy.[31,32] For the second region, ($\alpha < l0^4\,\mathrm{cm}^{-1}$), the absorption at the lower photon energy usually follows Urbach's rule $\alpha(\nu) = \alpha_0 \exp(h\nu/E_u)$, where ν is the frequency of the radiation, α_0 is a constant, h is the Planck constant, and E_u is Urbach's energy, which is interpreted as the width of the tails of localized states in the band gap of amorphous semiconductors. Figure 5(b) shows the variation of $\ln\alpha$ of the as-deposited films and post-annealing temperatures at 400, 500 and 600 as a function of the incident photon energy. By fitting data to a straight line, E_u can be determined. We find that Urbach's energy E_u for the as-deposited films and for the films with the post-annealing temperatures 400, 500, 600℃ are 1.85, 1.72, 1.61 and 1.38 eV, respectively. It is observed that E_u decreases with increasing the annealing temperature owing to the decrease of the width of localized states tail in the band gap.

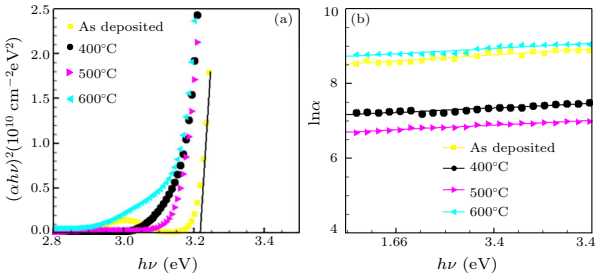

Fig. 5. Variation of $(\alpha h\nu)^2$ (a) and $\ln\alpha$ (b) of films versus $h\nu$.

Table 1. The different values of optical band gap of films.

Annealing temperature (℃)	E_g (eV)				
	Tauc model	$dR/d\lambda$	$dT/d\lambda$	Optical conductivity	WDD
As-deposited	3.21	3.24	3.21	3.31	3.05
400	3.15	3.23	3.2	3.27	2.9
500	3.16	3.12	3.19	3.28	2.9
600	3.14	3.2	3.22	3.26	2.63

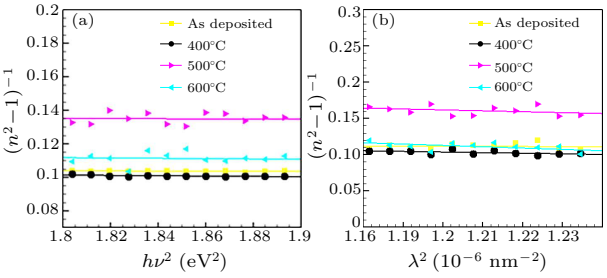

Fig. 6. The plots of $(n^2-1)^{-1}$ of films versus $(h\nu)^2$ (a) and λ^{-2} (b).

In the normal dispersion region, the refractive index dispersion can be analyzed by the single-oscillator model proposed by WDD:[33,34] $n^2 = 1 + (E_d E_0)/(E_0^2 - (h\nu)^2)$, where n is the refractive index, h is Planck's constant, ν is the frequency, $h\nu$ is the photon energy, E_0 is the average excitation energy for electronic transitions, and E_d is the dispersion energy. Figure 6(a) shows the plots of $1/(n^2-1)$ with $(h\nu)^2$ for as-deposited films and post-annealing temperatures at 400, 500 and 600℃. By fitting data in these plots to straight lines and from the intercepts E_0/E_d and slopes $1/E_0E_d$, E_0 and E_d can be determined. Furthermore, as proposed by Tanaka, the first approximate value of the optical band gap E_g^{opt} is also derived from the WDD model and is given by $E_g^{opt} \approx E_0/2$. Obviously, this value is almost in agreement with the optical band gap obtained from the other models. The

static refractive index n_0 for the films is calculated using the incident photon energy equal zero and is given by $n_0 = (1 + E_d/E_0)^{1/2}$. There is also an important parameter called the oscillator strength f, which is reported as $f = E_d E_0$.

Average oscillator wave length λ_0 and oscillator length strength S_0 for the as-deposited films and for the films with post-annealing temperatures at 400, 500 and 600℃ can be determined using the following relationship: $n^2 - 1 = S_0\lambda_0^2/(1 - (\lambda_0/\lambda)^2$, where $S_0 = (n_0^2 - 1)/\lambda_0^2$. Figure 6(b) shows the plots of $1/(n^2 - 1)$ with λ^{-2} for the as-deposited films and for the films with post-annealing temperatures 400, 500 and 600℃. By fitting data in these plots to straight lines, λ_0 and S_0 of the films are calculated.

The optical moments M_{-1} and M_{-3} of the optical spectra for the annealed films can be written as

$$E_0 = M_{-1}/M_{-3}, \quad E_d^2 = M_{-1}^3/M_{-3}.$$

The dispersion parameters obtained from the WDD model are listed in Table 2.

Table 2. The Wemple–Didomenico optical dispersion parameters of the films.

Annealing temperature (℃)	E_0 (eV)	E_d (eV)	λ_0 (10^3 nm)	n_0	M_{-1}	M_{-3} (eV^{-2})	S_0 (10^{-10} nm^{-2})	$f = E_0E_d$ (eV^2)
As-deposited	6.1	58.54	30	3.27	9.59	0.25	100.7	357.14
400	5.8	57.39	105	3.29	9.88	0.29	8.9	333.33
500	5.81	43	125	2.89	7.39	0.21	7.4	250
600	5.2	47.37	188	3.15	8.97	0.32	2.5	250

In summary, it is observed that the optical properties of the as-deposited films and the films with post-annealing temperatures 400, 500 and 600℃ can be strongly affected by annealing temperatures. The optical dispersion parameters are calculated by the Wemple–Didomenico model. It is shown that the optical band gap obtained by optical conductivity, $dR/d\lambda$, $dT/d\lambda$ and WDD analyses are in conformity with indirect optical band gap calculated using the Tauc model. With increasing the annealing temperature up to 500℃, the $dR/d\lambda$ and $dT/d\lambda$ peaks exhibit red shifts, while from 500 to 600℃ the peaks exhibit blue shifts. It is observed that the films annealed at 600℃ have the minimal indirect band gap at about 3.2 eV. The films annealed at 600℃ have minimal disorder. It is found that the dispersion energy E_d of films annealed at 500℃ has the minimum value of 43 eV.

References

[1] Zang Z, Wen M, Chen W et al 2015 *Mater. Des.* **84** 418
[2] Zang Z and Tang X 2015 *J. Alloys Compd.* **619** 98
[3] Sun Y, Riley D J and Ashfold M N R 2006 *J. Phys. Chem. B* **110** 15186
[4] Jin P, Nakao S, Wang S X et al 2003 *Appl. Phys. Lett.* **82** 1024
[5] Henley S J, Ashfold M N R and Cherns D 2004 *Surf. Coat. Technol.* **271** 177
[6] Duan L B, Zhao X R, Liu J M et al 2012 *Phys. Scr.* **85** 035709
[7] Liang Z, Yu X, Lei B et al 2011 *J. Alloy. Compd.* **509** 5437
[8] Cho S, Ma J, Kim Y et al 1999 *Appl. Phys. Lett.* **75** 2761
[9] Chen H, Jin H J and Park C B 2009 *Electr. Electron. Mater.* **10** 93
[10] Dalouji V and Asareh N 2017 *Opt. Quantum Electron.* **49** 262
[11] Dalouji V, Elahi S M and Ahmadmarvili A 2017 *Silicon* **9** 717
[12] Dalouji V and Elahi S M 2016 *Surf. Rev. Lett.* **23** 1650002
[13] Dalouji V 2016 *Mater. Sci.-Poland* **34** 337
[14] Dalouji V, Elahi S M, Ghaderi A et al 2016 *Chin. Phys. Lett.* **33** 057203
[15] Dalouji V, Elahi S M, Solaymani S et al 2016 *Appl. Phys. A* **122** 541
[16] Ţălu Ş Bramowicz M, Kulesza S et al 2016 *Microsc. Res. Tech.* **79** 1208
[17] Ţălu Ş Bramowicz M, Kulesza S et al 2016 *J. Microsc.* **264** 143
[18] Ghodselahi T, Solaymani S, Akbarzadeh P M et al 2012 *Eur. Phys. J.* D **66** 299
[19] Dalouji V, Elahi S M, Solaymani S et al 2016 *Eur. Phys. J. Plus* **131** 84
[20] Abbas M M, Shehab A A, Al-Samuraee A K et al 2011 *Energ. Procedia* **6** 241
[21] Metin H and Esen R 2003 *Erciyes University Fen Bilimeri Enstitusu Dergisi* **19** 96
[22] Farag A A M, Cavas M, Yakuphanoglu F et al 2011 *J. Alloys Compd.* **509** 7900
[23] Sakr G B, Yahia I S, Fadel M et al 2010 *J. Alloys Compd.* **507** 557
[24] Fujii T, Nishikiori H and Tamura T 1995 *Chem. Phys. Lett.* **233** 424
[25] Gagandeep S K, Lark B S and Sahota H S 2000 *Nucl. Sci. Eng.* **134** 208
[26] Sharma P and Katyal S C 2008 *Mater. Chem. Phys.* **112** 892
[27] Pejova B and Grozdanov I 2001 *J. Solid State Chem.* **158** 49
[28] Kenny N, Kannewurf C R and Whitmore D H 1966 *J. Phys. Chem. Solids* **27** 1237
[29] Mott N F, Davis E A 1979 *Electronic Process in NonCrystalline Materials* (Oxford: Calendron Press)
[30] Khan S A, Lal J K and AlGhamd A A 2010 *Opt. Laser Technol.* **42** 839
[31] Shan F K, Liu G X, Lee W J et al 2007 *J. Appl. Phys.* **101** 053106
[32] Cohen M H, Fritzsche H and Ovshinsky S R 1969 *Phys. Rev. Lett.* **22** 1065
[33] Wemple S H and Didomenico M 1971 *J. Phys. Rev.* B **3** 1338
[34] Wemple S H and Didomenico M 1973 *J. Phys. Rev.* B **7** 3767